

**SOL-GEL COATINGS WITH IF-WS<sub>2</sub> ON ALUMINUM OXIDE LAYER**Joanna KORZEKWA <sup>1</sup>, Grzegorz DERCZ <sup>2</sup>, Paweł WIECZOREK <sup>3</sup>, Aneta GADEK-MOSZCZAK <sup>4</sup>

<sup>1</sup>University of Silesia, Faculty of Computer and Materials Science,  
ul. Żytnia 10, 41-200 Sosnowiec, Poland, EU, [joanna.korzekwa@us.edu.pl](mailto:joanna.korzekwa@us.edu.pl)

<sup>2</sup>University of Silesia, Faculty of Computer and Materials Science,  
ul. 75 Pułku Piechoty 1A, 41-500 Chorzów, Poland, EU, [grzegorz.dercz@us.edu.pl](mailto:grzegorz.dercz@us.edu.pl)

<sup>3</sup>Czestochowa University of Technology, Faculty of Production Engineering and Materials Technology,  
Al. Armii Krajowej 19, 42-200 Czestochowa, Poland, EU, [pawel@wip.pcz.pl](mailto:pawel@wip.pcz.pl)

<sup>4</sup>Cracow University of Technology, Faculty of Mechanical Engineering,  
Al. Jana Pawła II 37, 31-864 Krakow, Poland, EU, [aneta.gadek-moszczak@mech.pk.edu.pl](mailto:aneta.gadek-moszczak@mech.pk.edu.pl)

**Abstract**

The hybrid coatings prepared on aluminum substrates were the object of a study of their tribological properties. An amorphous oxide layers Al<sub>2</sub>O<sub>3</sub> were obtained on aluminum alloy EN AW 5251. The top coatings were sol-gel matrices with embedded nanoparticles of inorganic fullerene-like tungsten disulfide IF-WS<sub>2</sub>. The coatings were coupled with two kinds of plastic TG15 and PEEK/BG in order to measure their tribological properties as wear intensity and friction coefficient. Scanning electron microscope and surface adhesion were also studied.

**Keywords:** Composite coatings, sol-gel method, inorganic fullerene-like tungsten disulfide, tribological properties

**1. INTRODUCTION**

Aluminium alloys belong to a group of materials which are widely used in motorization, aircraft or food industry, where light weight or corrosion resistance is required. The anodic aluminum oxide (AAO) coatings, made on the substrate of aluminum alloys, are particularly useful as protective coatings in varied application. By molding the AAO on the substrate of aluminum alloys during the anodic oxidation process, we obtain the material with improved hardness, which is corrosion resistant with good wear properties. In recent years many studies have been focus on modification of AAO and aluminium alloy. One of these methods is sol-gel protective coatings which can improve corrosion resistance of alloy surface in various corrosion mediums and practical application [1]. Sol-gel protective coating are also environmentally friendly and then they are interesting as replacements for chromium based conversion coatings. Conde at al. [2] prepared sol-gel corrosion protective coatings on aluminium alloy using spin coating method. Fori at al. [3] showed the colloidal suspension conductivity is a key parameter in electrophoretic deposition of nanoparticles inside a AAO. Liu at al. [4] explored titanium coatings on anodized aluminum surface which were obtained by a vacuum dip-coating method in TiO<sub>2</sub> colloidal solution. They proved that such coatings effectively inhibit the aluminum corrosion in sterile seawater. The analyze of interaction between silane based sol-gel chemistries and anodised layer including the pore penetration and compare corrosion performance on different anodised aluminium layers were done by Whelan [5]. Kumar at al. [6] proposed one-step anodization/sol-gel deposition of cerium doped silica-zirconia coatings on aluminium. Those investigations mainly paid attention to corrosion protection or optical investigation or current/voltage studies. Despite the breadth of research concerning sol-gel coatings and also an information about limitation of adhesion of inorganic coatings, to the best of our knowledge little research has been published in term of tribological properties of such coatings. The objective of the present work is to investigate the tribological and physical and chemical properties of Al<sub>2</sub>O<sub>3</sub>/IF-WS<sub>2</sub> coatings obtained by sol-gel method. To this purpose microstructural analysis, X-ray diffraction, tribological tests and adhesion tests were conducted.

## 2. MATERIALS AND METHODS

### 2.1. Experimental

The substrate under a colloidal solution of IF-WS<sub>2</sub> coating was an amorphous Al<sub>2</sub>O<sub>3</sub> oxide layer obtained on aluminum alloy. The Al<sub>2</sub>O<sub>3</sub> oxide layer was obtained on aluminum alloy EN AW 5251 via electro-oxidation method route, which is described elsewhere [7] as a first step. The 3-glycidoxypropyltrimethoxysilane C<sub>9</sub>H<sub>20</sub>O<sub>5</sub>Si (GLYMO, Sigma Aldrich), aqueous colloidal silica SiO<sub>2</sub> (LUDOX 34 wt.%, Sigma Aldrich), ethanol C<sub>2</sub>H<sub>5</sub>OH and distilled water H<sub>2</sub>O, in the molar ratio: 0.15:0.5:0.5:2.5 was used to prepare the solution of organic precursor. The 5 % of inorganic fullerene-like nanoparticles of tungsten disulfide IF-WS<sub>2</sub> (NanoMaterials Ltd) with respect to the total weight of the solution were added. The solution of organic and inorganic network were mixed and hydrolyzed by 1 hour in 50 ± 1 °C using magnetic stirrer with speed of 600 rpm/min. The substrate sheet of 10<sup>-3</sup> m<sup>2</sup> size was dip-coated in sol. In to better homogenization and dispersion of IF-WS<sub>2</sub> the ultrasound treatment was used by 30 min. The samples were thermally treated at 150 °C in air.

### 2.2. Microstructural characterization

The worn surfaces and fresh cross-section structures of the layers were analyzed by a HITACHI S 4700 scanning electron microscope (SEM) with a NORAN Vantage digital energy dispersive X-ray microanalysis (EDS) system. In order to analyze the surface and fresh cross section of the samples were coated by carbon coating (sample xC) using thermal evaporation technique - Cressington Carbon Coater 208, time 2 x 20-30 seconds, current 80-100 A.

### 2.3. Tribological properties measurements

Tribological measurements were performed on a T17 tester, a pin-on-plate in a reciprocating motion, at room temperature, at the humidity of 30 ± 5 %, using 0.5 MPa pressure at an average sliding speed of 0.2 m/s in dry friction conditions. The tribological test was conducted for sliding distance of 15 km. The commercial TG15 and PEEK/BG plastic pins of a 9 x 10<sup>-2</sup> dm in diameter were used as a counter-body. The plastic TG15 is a modified version of the standard PTFE (polytetrafluoroethylene), which was filled with graphite. The percentage of added graphite is in the range 15-30 %. The TG15 material is mainly used in heavy-duty slide bearings. It is also used in the production of machine parts (bearings and other sliding elements), the production of anti-corrosion coatings, insulation, sealing components and valve parts. The counter specimen PEEK/BG is polyetheretherketone with PTFE, graphite and carbon fibers of Erta. The friction coefficient was measured when a steady state was reached in the friction test. The wear quantity of the TG15 and PEEK/BG plastics was studied by using a WA32 analytical balance with the accuracy of 0.1 mg, after each friction process.

### 2.4. X-ray diffraction measurements

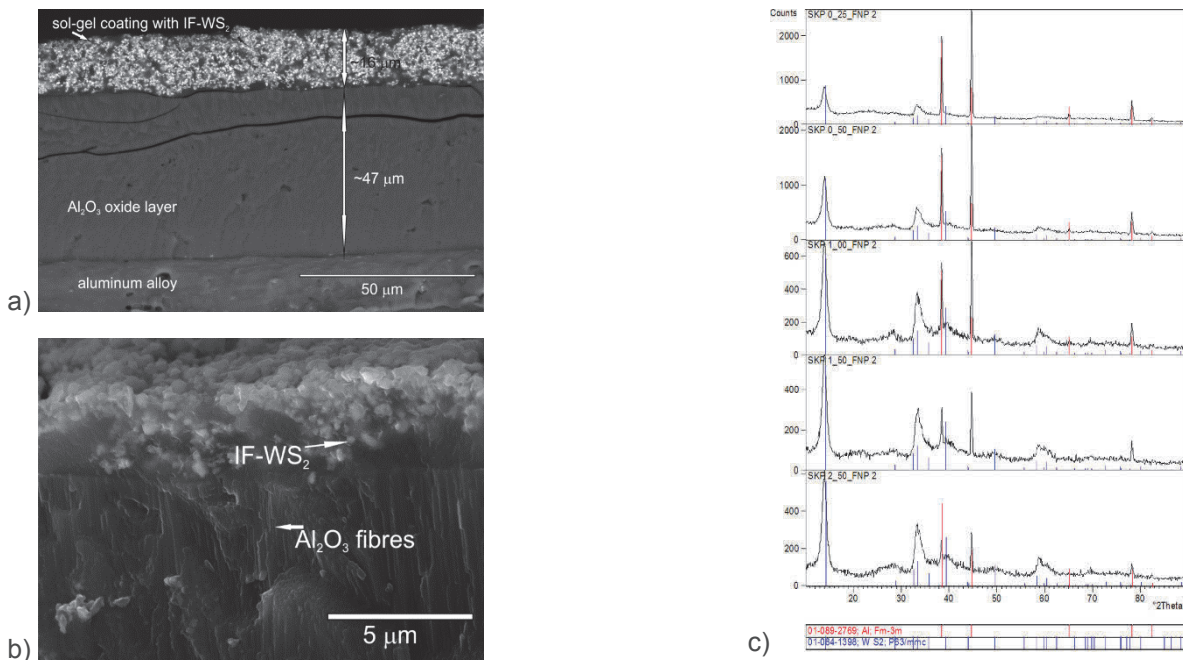
X-ray diffraction (XRD) experiments were performed on an X'Pert Philips PW 3040/60 diffractometer operating at 30 mA and 40 kV, which was equipped with a vertical goniometer and Eulerian cradle. The wavelength of the radiation ( $\lambda_{\text{CuK}\alpha}$ ) was 1.54178 Å. Grazing angle incidence X-ray diffraction (GIXD) patterns were registered in the 2 $\theta$  range from 10° to 90° with a 0.05° step for the incident angles: 0.25°, 0.50° and 1.00°. At low  $\alpha$  angles of incidence, the X-rays penetrate only the uppermost layers of a sample. At higher  $\alpha$  angles of incidence, the X-rays penetrate deeper into the sample. To maintain comparable intensities of the diffraction lines, the conditions for collecting the pattern (step and counting time) were properly adjusted.

### 2.5. Adhesion test

The adhesion test were carried out on an automated Revetest Xpress Plus instrument using a diamond Rockwell intender [8]. The following parameters were used: preset load of 1-75 N, scratch 15 mm, load increased 50 N/min. Microscopic observation of scratch surface and penetration depth were analyzed.

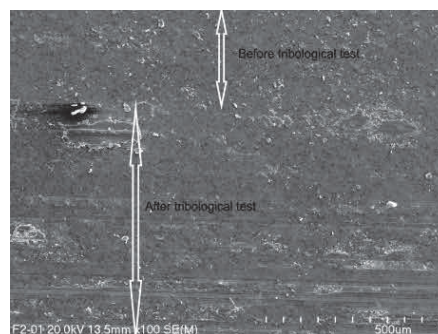
### 3. RESULTS AND DISCUSSION

The fresh cross section of Al<sub>2</sub>O<sub>3</sub> oxide layers with sol-gel IF-WS<sub>2</sub> coatings is shown in **Figure 1a** (magnification x1000) and **Figure 1b** (magnification x5000). The **Figure 1c** shows XRD diffraction pattern of layer presents in **Figure 1a** and **Figure 1b**. The summary of GIXD diffraction patterns obtained by the test indicates that the crystalline phase contains layers of aluminum. Additionally, the presence of IF-WS<sub>2</sub> modifier was revealed and so-called X-ray "amorphous halo" indicates that part of the material is in the amorphous form. Detailed analysis of the diffraction patterns obtained by GIXD method showed that with the increase of the beam angle ( $\alpha$ ), the phases are changed. For the lowest value of  $\alpha = 0.25^\circ$ , so the top layer, the crystalline phase Al have the largest share. A further increase in the angle of the beam to  $\alpha = 2.50^\circ$  reveals the disorders of the crystalline unit cell.



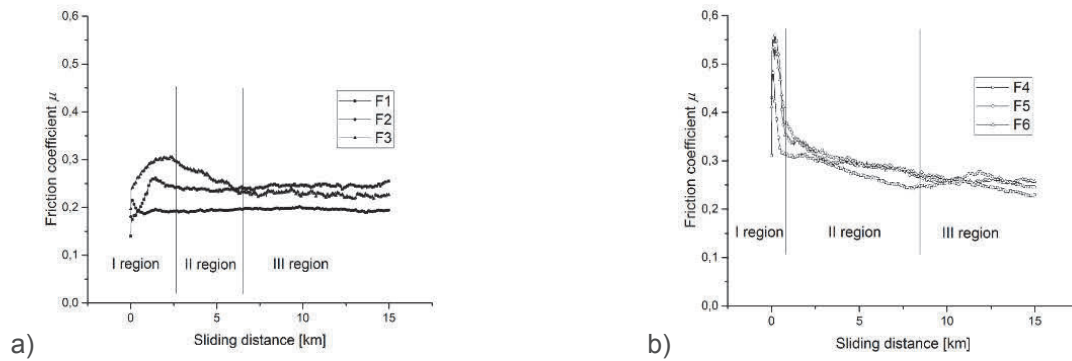
**Figure 1** SEM images of fresh cross section: a) zoom x1000 (left), b) zoom x5000 (right), c) XRD spectra of Al<sub>2</sub>O<sub>3</sub> - sol gel IF-WS<sub>2</sub> layer.

The **Figure 2** shows the surface of sample before and after tribological test with TG15 plastic. There is visible that sol-gel IF-WS<sub>2</sub> coating is continuous and uninterrupted as well as before and after tribological test. As a result of friction force the sliding film consists of TG15 and IF-WS<sub>2</sub> particle was created. The sol-gel layer of IF-WS<sub>2</sub> is not removed from the surface of the oxide, but rather under the plastic load of the plastic mandrel, it is rubbed into the surface of the oxide.



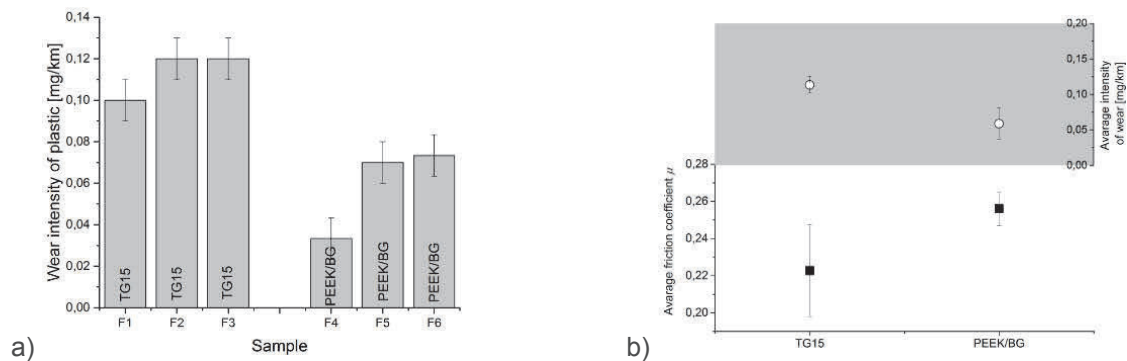
**Figure 2** Image of the surface samples after and before tribological test.

In order to tribological test the three of samples were conducted with TG15 and PEEK/BG counters-body. The results of tribological test are presented in **Figure 3a** with TG15 and **Figure 3b** with PEEK/BG. The first region, when a sudden increase in the friction coefficient is present, is created due to the initial contact between the pin and the sample. In case of TG plastic the distance for this region is about 2.5 km, while for PEEK/BG is about 0.8 km. The second region of the displacement a diminution is present due to a more flat surface, and finally in region three when the coefficient is stable.



**Figure 3** Dependence of friction coefficient vs sliding distance:  
(a) for samples conducted with TG15, (b) for samples conducted with PEEK/BG.

The graph (**Figure 4**) reveals a slight increase in the friction coefficient that is associated with a process of micro-welding that are formed and destroyed as the pin slips on the probe and as the material wear out allowing the formation of new surfaces. These new surfaces have a tribological behavior different from that of the original surface.

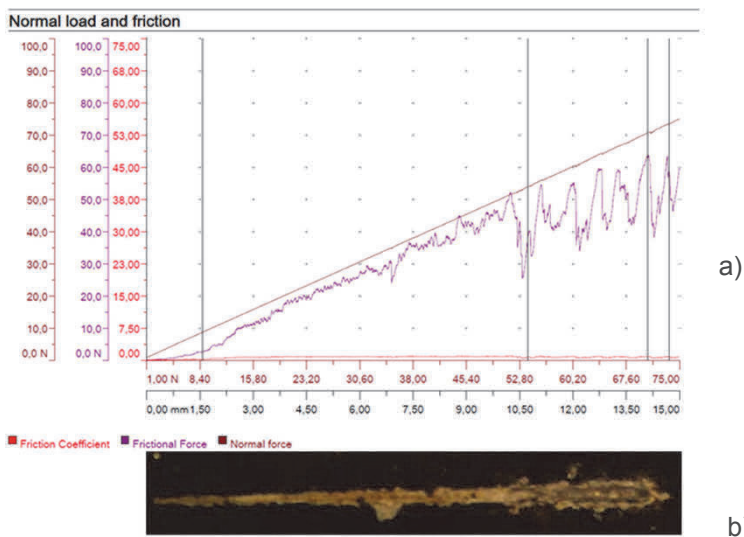


**Figure 4** Wear intensity for different samples (a) and average friction coefficient for different materials (b)

The mechanical properties of the coating have been measured on the basis of a visual assessment of the crack's perceptibility. Five replicated measurements were made and the results are presented in **Table 1**. **Figure 5a** shows a sample of the dependence of the friction force and normal force on the scratch length. **Figure 5b** shows a picture of a scratch made on a sample. The variability of the friction force, during normal force build-up in relation to the length of the crack, allowed to determine the characteristic points indicating the deformation of the tested surface. The adhesion test provided conclusions regarding both the IF-WS<sub>2</sub> surface layer and the oxide layer obtained on the aluminum alloy. Under the pressure of the Rockwell indenter, the outer layer of IF-WS<sub>2</sub> was destroyed at the initial force of 1N. The average pressure force of approx. Lcc = 11 N may already cause the first cohesive crack in the oxide coating. With an average value of the pressure force Lca = 57 N, the first adhesive cracks appear on the layer showing the aluminum alloy substrate on which the oxide layer was formed.

**Table 1** Scratch test measurements

Scratch number	1	2	3	4	5	Mean
Cohesive force Lcc (N)	13.42	10.22	8.78	15.91	8.86	11.43 ± 3.13
Adhesive force Lca (N)	48.60	56.12	53.88	39.36	36.27	46.85 ± 8.75


**Figure 5** The dependence of the friction force and normal force on the scratch length.

#### 4. CONCLUSION

As a result of the technological process, the hybrid coatings of colloidal solution of IF-WS<sub>2</sub> and an amorphous Al<sub>2</sub>O<sub>3</sub> oxide layer were obtained on aluminum alloy. The tribological tests showed comparable (including deviations) friction coefficient between the coatings and TG15 and PEEK/BG materials, whose average values were about 0.22 and 0.26 respectively. As a result of micro-welding a sliding film of the sol-gel layer and plastic material were formed. These new surfaces have a tribological behavior different from that of the original surface. Adhesion tests showed that the diamond Rockwell intender destroyed the sol-gel layer already at a force of about 1N, while the oxide layer withstands a load of 57 N. Above this value the oxide layer were destroyed. It will be worth to use, in further investigation, some interesting analytical methods from a materials science [9-14] combined with specific applications of the multivariate analysis [15-21] and an image analysis [22-25].

#### REFERENCES

- [1] WANG, D. and BIERWAGEN, G.P. Sol-gel coatings on metals for corrosion protection, *Prog. Org. Coat.* 2009, vol. 64, pp. 327-338.
- [2] CONDE, A., DURÁN, A. and DAMBORENEA, J.J. Polymeric sol-gel coatings as protective layers of aluminium alloys, *Prog. Org. Coat.* 2003, vol. 46, pp.288-296.
- [3] FORI, B., TABERNA, P.L., ARURAUULT, L. and BONINO, J.P. Decisive influence of colloidal suspension conductivity during electrophoretic impregnation of porous anodic film supported on 1050 aluminium substrate. *J. Colloid Interface Sci.* 2014, vol. 413, pp.31-36.
- [4] LIU, T., ZHANG, F.F., XUE, C.R., LI, L. and YIN, Y.S. Structure stability and corrosion resistance of nano-TiO<sub>2</sub> coatings on aluminum in seawater by a vacuum dip-coating method. *Surf. Coat. Technol.* 2010, vol.205, pp.2335-2339.

- [5] WHELAN, M., CASSIDY, J. and DUFFY, B. Sol-gel sealing characteristics for corrosion resistance of anodised aluminium. *Surf. Coat. Technol.* 2013, vol.235, pp.86-96.
- [6] N. KUMAR, A. JYOTHIRMAYI, K. R. C. SOMA RAJU, V. UMA, and R. SUBASRI. One-Step Anodization/Sol-Gel Deposition of -Doped Silica-Zirconia Self-Healing Coating on Aluminum. *ISRN Corrosion*, Volume 2013, Article ID 424805, 8 pages
- [7] KORZEKWA, J., TENNE, R., SKONECZNY, W. and DERDZ, G. Two-step method for preparation of Al<sub>2</sub>O<sub>3</sub>/IF-WS<sub>2</sub> nanoparticles composite coating. *Phys. Status Solidi A-Appl. Mat.* 2013, vol.210, pp. 2292-2297.
- [8] GWOŹDZIK, M. and NITKIEWICZ, Z. Studies on the adhesion of oxide layer formed on X10CrMoVNb9-1 steel. *Arch. Civ. Mech. Eng.* 2014, vol. 14, pp.335-341.
- [9] DEFLORIAN, F., CIAGHI, L. and KAZIOR, J. Electrochemical characterization of vacuum sintered copper alloyed austenitic stainless-steel. *Werkst. Korros.-Mater. Corros.* 1992, vol.43, pp.447-452.
- [10] ŻÓRAWSKI, W., CHATYS, R., RADEK, N. and BOROWIECKA-JAMROŹEK, J. Plasma-sprayed composite coatings with reduced friction coefficient. *Surf. Coat. Technol.* 2008, vol.202, pp.4578-4582.
- [11] SZCZOTOK, A. and RODAK, K. Microstructural studies of carbides in MAR-M247 nickel-based superalloy. *IOP Conference Series-Materials Science and Engineering* 2012, vol.35, art. 012006.
- [12] ŹENKIEWICZ, M., ŹUK T. and PIETRASZEK, J. Modeling electrostatic separation of mixtures of poly(ε-caprolactone) with poly(vinyl chloride) or poly(ethylene terephthalate). *Przemysł Chemiczny.* 2016, vol.95, pp.1687-1692.
- [13] SZCZOTOK, A., PIETRASZEK, J. and RADEK, N. Metallographic study and repeatability analysis of γ' phase precipitates in cored, thin-walled castings made from IN713C superalloy. *Arch. Metall. Mat.* 2017, vol.62, pp.595-601.
- [14] PIETRASZEK, J., SZCZOTOK, A. and RADEK, N. The fixed-effects analysis of the relation between SDAS and carbides for the airfoil blade traces. *Arch. Metall. Mat.* 2017, vol.62, pp.235-239.
- [15] PIETRASZEK, J., SZCZOTOK, A. and KOCYŁOWSKA E. Factorial approach to assessment of GPU computational efficiency in surrogate models. *Adv. Mat. Res.-Switz.* 2014, vol.874, pp.157-162.
- [16] PIETRASZEK, J. and GOROSHKO, A. The Heuristic Approach to the Selection of Experimental Design, Model and Valid Pre-Processing Transformation of DoE Outcome. *Adv. Mat. Res.-Switz.* 2014, vol.874, pp. 145-149.
- [17] PIETRASZEK, J. and SKRZYPCZAK-PIETRASZEK, E. The Optimization of the Technological Process with the Fuzzy Regression. *Adv. Mat. Res.-Switz.* 2014, vol. 874, pp. 151-155.
- [18] LISOWSKI, E. and FILO, G. Automated heavy load lifting and moving system using pneumatic cushions. *Autom. Constr.* 2015, vol.50, pp.91-101.
- [19] PIETRASZEK, J., KOŁOMYCKI, M., SZCZOTOK, A. and DWORNICKA, R. The Fuzzy Approach to Assessment of ANOVA Results. *Lecture Notes in Computer Science* 2016, vol 9875, pp.260-268.
- [20] LISOWSKI, E. and FILO, G. Analysis of a proportional control valve flow coefficient with the usage of a CFD method. *Flow Meas. Instrum.* 2017, vol.53, pp.269-278.
- [21] SKRZYPCZAK-PIETRASZEK, E., KWIECIEŃ, I., GOŁDYN, A. and PIETRASZEK, J. HPLC-DAD analysis of arbutin produced from hydroquinone in a biotransformation process in *Origanum majorana* L. shoot culture. *Phytochem. Lett.* 2017, vol.20, pp.443-448.
- [22] KOZIEN, M. Acoustic intensity vector generated by vibrating set of small areas with random amplitudes. *J. Theor. Appl. Mech.* 2009, vol.47, pp.411-420.
- [23] KORZEKWA, J., GADEK-MOSZCZAK, A. and BARA, M. The Influence of Sample Preparation on SEM Measurements of Anodic Oxide Layers. *Prakt. Metallogr.-Pract. Metallogr.* 2016, vol.53, pp. 36-49.
- [24] GADEK-MOSZCZAK, A. History of stereology. *Image Anal. Stereol.* 2017, vol. 36, pp.151-152.
- [25] GADEK-MOSZCZAK, A. and MATUSIEWICZ, P. Polish stereology - a historical review. *Image Anal. Stereol.* 2017, vol. 36, pp.207-221.